Němec, D., 2026. Recent microphysics developments in the ALARO model. In: Tolasz, R., Šustková, V. (Ed.), Proceedings of the 2nd PERUN Project Conference (TA ČR, SS02030040). CHMI, Praha, pp. 54–61, ISBN 978-80-7653-095-9. https://doi.org/10.59984/978-80-7653-095-9.07

Recent microphysics developments in the ALARO model

(Nedávné změny v mikrofyzice modelu ALARO)

Němec, D.

David Němec, Czech Hydrometeorological Institute; Faculty of Mathematics and Physics, Charles University, david.nemec@chmi.cz

https://doi.org/10.59984/978-80-7653-095-9.07

Abstract: Parameterizations of microphysics of clouds and precipitation differ in their complexity. While many climate models rely on single-moment schemes, which predict prognostically only the mass of hydrometeors, double-moment schemes add the number concentration as a prognostic model variable. Consequently, they can distinguish small raindrops originating from the collision-coalescence process from usually bigger raindrops from the melting of ice particles. The current single-moment scheme of the ALARO model is extended to a double-moment scheme for selected hydrometeors, enabling the use of more sophisticated parameterizations for processes, changing their fluxes. In addition, new processes are integrated into the scheme, which are related to the more complex description of the hydrometeor development or are related only to double-moment schemes, as they affect only hydrometeor number concentration. Next, the characteristics of the model simulations with the new scheme are discussed. The ability of the scheme to generate realistic rain number concentrations across various weather regimes is validated using disdrometer measurements. Finally, the typical characteristics of the scheme regarding the precipitation field are shown, along with how the typical vertical velocities in updrafts are shifted.

Keywords: parametrization – microphysics of clouds and precipitation – double-moment scheme – disdrometer

Abstrakt: Parametrizace mikrofyziky oblaků a srážek se liší svou komplexností. Zatímco mnohými klimatickými modely využívaná jednomomentová schémata určují prognosticky pouze hmotnost hydrometeorů, dvoumomentová schémata přidávají jako prognostickou veličinu jejich početní koncentraci. Díky tomu mohou například rozlišit původ malých dešťových kapek vzniklých kolizně-koalescenčním procesem od obvykle větších kapek vzniklých táním ledových částic. Současné jednomomentové schéma modelu ALARO je postupně rozšiřováno na dvoumomentové pro vybrané hydrometeory. To umožňuje použití sofistikovanějších parametrizací některých procesů. Díky tomu je značně změněna jejich rychlost. Dále jsou do schématu zavedeny nové procesy, které souvisí buď s komplexnějším popisem tvorby hydrometeorů, či jsou využitelné jen pro dvoumomentová schémata, neboť ovlivňují pouze početní koncentraci. Další část je věnována validaci a ukázce vlastností nového schématu. Pomocí měření z disdrometrů bude otestováno, zdali je schéma schopno vytvářet realistické množství dešťových kapek v různých režimech počasí. Na závěr jsou ukázány charakteristické rysy schématu týkající se srážkového pole a typických konvektivních výstupných rychlostí.

Klíčová slova: parametrizace – mikrofyzika oblaků a srážek – dvojmomentové schéma – disdrometer

Introduction

Microphysics schemes are one of the essential parameterizations in climate models. They are responsible for the creation and evolution of precipitation, one of the elemental meteorological and climatological quantities. Despite the impact on future climate and society, the description of microphysical processes remains highly uncertain, and their parameterizations pose a challenging task in climate modeling.

Various microphysics schemes have been developed, differing in their complexity. Many current climate models use single-moment schemes (Daniel et al. 2019; Remedio et al. 2019; Sørland et al. 2021). Such schemes compute the evolution of hydrometeor mass. Other quantities, such as the number concentration, are computed diagnostically based on the prescribed hydrometeor size distribution.

The increase in computational power will enable the use of more sophisticated physics parameterizations in the future. One such category are the double-moment schemes, which add a new prognostic for the hydrometeor number concentration. The single-moment and double-moment approaches can be combined by computing two prognostic moments for some hydrometeors while one for others (Thompson et al. 2008).

The current microphysics scheme used in the latest version of ALARO-climate is a single-moment one with five prognostic hydrometeors: cloud water, cloud ice, rain, snow, and graupel (Nemec et al. 2024). Each precipitating hydrometeor is assumed to follow a negative exponential distribution. The simulated processes are autoconversion, collection, evaporation, and melting. This scheme is incrementally extended for the second moment for selected hydrometeors.

This work concentrates on the extension to double-moment cloud water and rain. Their advancement to double-moment species requires introducing several new processes. Firstly, the number concentration of cloud droplets resulting from aerosol activation must be determined after the thermodynamic adjustment yields the mass fraction of cloud water. The activation of aerosols to determine the cloud water number concentration is parameterized following Feingold and Heymsfield 1992. This parametrization predicts the cloud water number concentration based on the temperature, aerosol concentration, and vertical velocity in the model gridbox. Since the current model version is non-hydrostatic with parameterized deep convection, two distinct vertical velocities are computed. Therefore, the activation is also separately computed for both vertical velocities. Then, the resulting number concentration is combined based on the amounts of the resolved and convective condensation fluxes. Secondly, the number concentration of cloud droplets can be reduced by self-collection. Finally, the self-collection and break-up of raindrops are other new processes.

The double-moment schemes can naturally include aerosol sensitivity to the microphysics. In this work, the aerosol field is provided by the monthly aerosol climatology of the Copernicus Atmospheric Monitoring Service (CAMS), which offers 11 aerosol species (Bozzo et al. 2020). The scheme is expected to allow the use of aerosols from more sources in the future.

Data

For the model simulations, the ALARO model is used (Termonia et al. 2018). The selected domain consists of 1069×853 points and covers Central Europe and adjacent areas. The time step is 90 s. The reference model configuration with the single-moment scheme is denoted by 1MOM, while 2LIQ denotes the configuration with the extension for double-moment cloud water and rain.

To validate the number concentration delivered by the single-moment and double-moment schemes, data from the Thies Clima Laser Precipitation Monitor (LPM) disdrometers at the Lindenberg and Muenchen-Stadt stations (Deutscher Wetterdienst et al. 2025) are used. The Thies LPM disdrometer measures 22 categories of diameters ranging from the smallest diameter category 0.125–0,250 mm to more than 8 mm and 20 categories of fall speeds ranging from the first category of 0–0.2 $m \cdot s^{-1}$ to more than 10 $m \cdot s^{-1}$. Consequently, the disdrometer cannot detect the smallest particles with diameters lower than 0.125 mm, which do not contribute significantly to mass or rainfall but can be abundant in number concentration. Therefore, the model data are cut according to their size distribution to match the same range of diameters to have comparable data. The data from disdrometers and the model are originally obtained every 3 minutes, but for this presentation, a 15-minute moving average is applied for readability.

Results

The comparison to the disdrometer data from a convective case at the Muenchen-Stadt station on 2024-07-06 from 12 to 24 UTC is depicted in Fig. 1. The onset of the precipitation is delayed in the model, but it does not change the precipitation characteristics much as the character of the meteorological situation is kept. The maximum precipitation rate is slightly lower in the model than in the disdrometer, with 1MOM slightly more underestimating than 2LIQ. The number concentration delivered by 2LIQ is comparable to that measured by the disdrometer, with both exceeding 7000 m^{-3}. However, 1MOM cannot deliver such high number concentrations and peaks at slightly over 2000 m^{-3}. The number concentration delivered by both model configurations is similar at lower precipitation rates. The mass-weighted fall speed of rain is overestimated at the onset of precipitation in 2LIQ because of too strong size-sorting. Both simulations are similar at higher precipitation rates and match the disdrometer-measured fall speeds well. Both simulations capture the radar reflectivity well, but 2LIQ shows greater variability, as observed with the disdrometer. The mean volume diameter (ratio of the third to the zeroth moment of the size distribution that all to the power of 1/3) and mass-weighted diameters (ratio of the fourth to the third moment of the size distribution) are overestimated during the onset of precipitation by 2LIQ, but comparable to 1MOM and the disdrometer for the rest of the time window. In this particular case, 1MOM fall speed matches the measured one better.

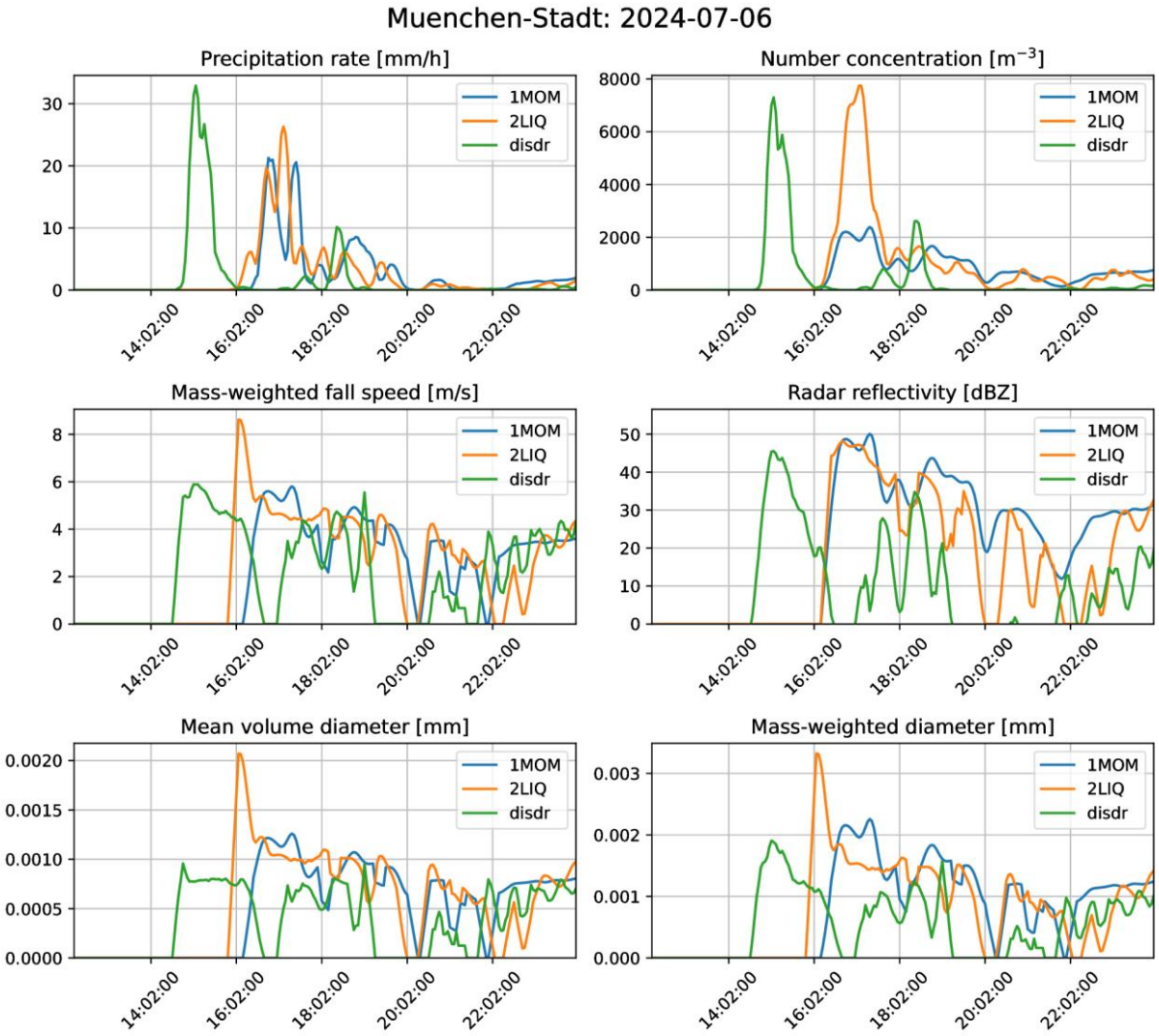


Fig. 1. Comparison of model to disdrometer data on 2024-07-06 at the Muenchen-Stadt station. 1MOM in blue, 2LIQ in orange, disdrometer in green.

Fig. 2 shows results for a large-scale precipitation case at the Lindenberg station on 2024-09-15 from 12 to 24 UTC. The precipitation rate is similar between the model and the disdrometer, although precipitation is observed before the modeled onset. Contrarily, both model simulations delay the termination of the main rain event. Again, the delay should not have any significant impact of the precipitation characteristics.

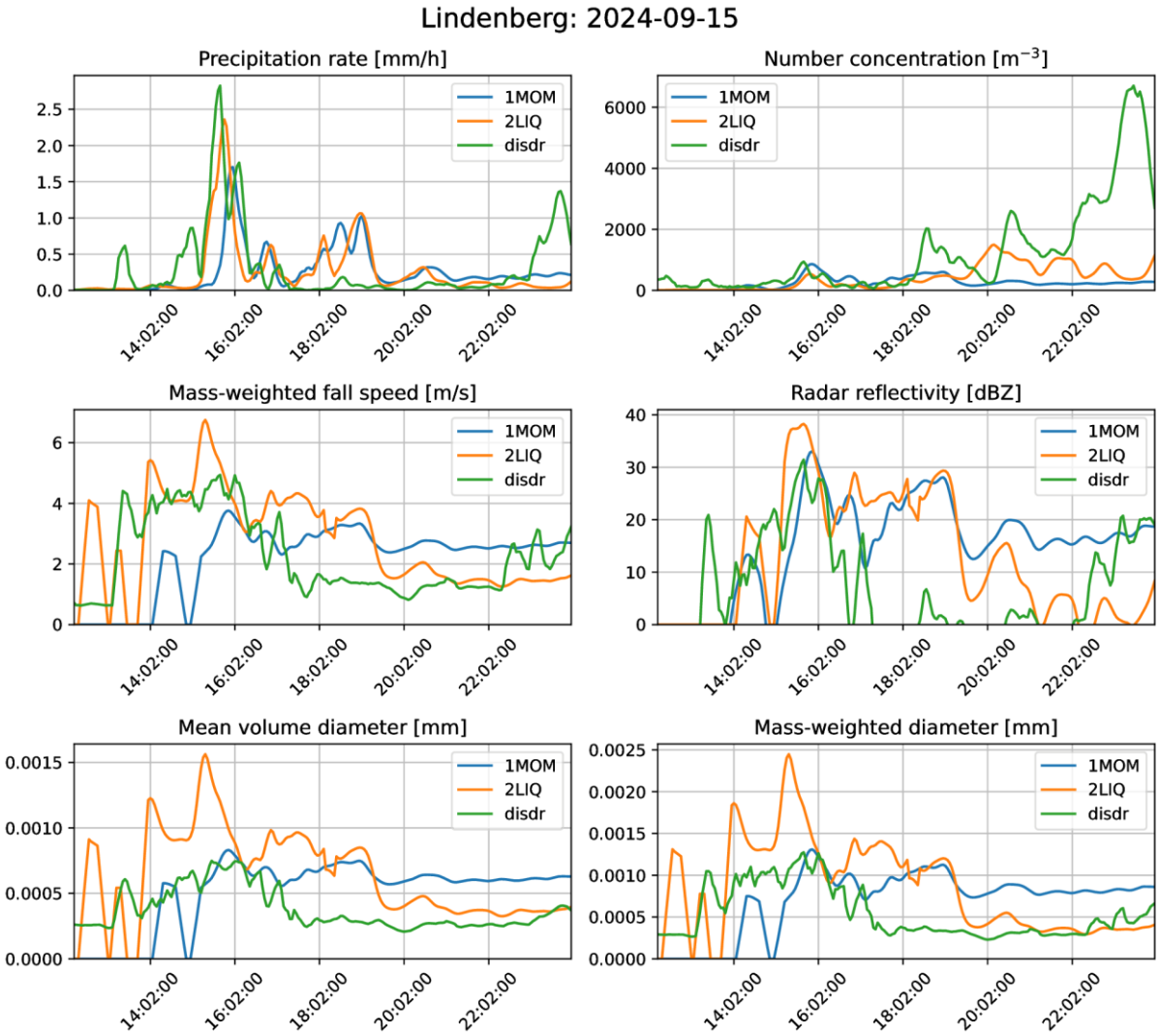


Fig. 2. Comparison of model to disdrometer data on 2024-09-15 at the Lindenberg station. 1MOM in blue, 2LIQ in orange, disdrometer in green.

Neither simulation captured the increase in precipitation rate observed by the disdrometer near the end of the time window. However, both simulations keep the precipitation pattern, which is important for the comparison. The number concentration evolution in 1MOM follows the prescribed distribution with lowering the number concentration with lower precipitation rates, whereas 2LIQ raises the number concentration towards the second half of the time window, showing a transition to smaller drops, as observed by the disdrometer. The mass-weighted fall speed is also decreased in 2LIQ in the last hours of the window, consistent with the tendency observed by the disdrometer. Conversely, the mass-weighted fall speed is too high in 2LIQ during the initial phase due to overly strong size sorting. The radar reflectivity remains too high in 1MOM, while decreasing in 2LIQ towards the end of the simulation; however, it is too high at the beginning of the rain event due to too large particles, which is confirmed by the mean volume diameter and mass-weighted diameter, which 2LIQ overestimate at the

beginning of the rain event. However, 2LIQ can capture the transition to smaller drops towards the end of the rain event, which 1MOM misses, as the drops remain too large.

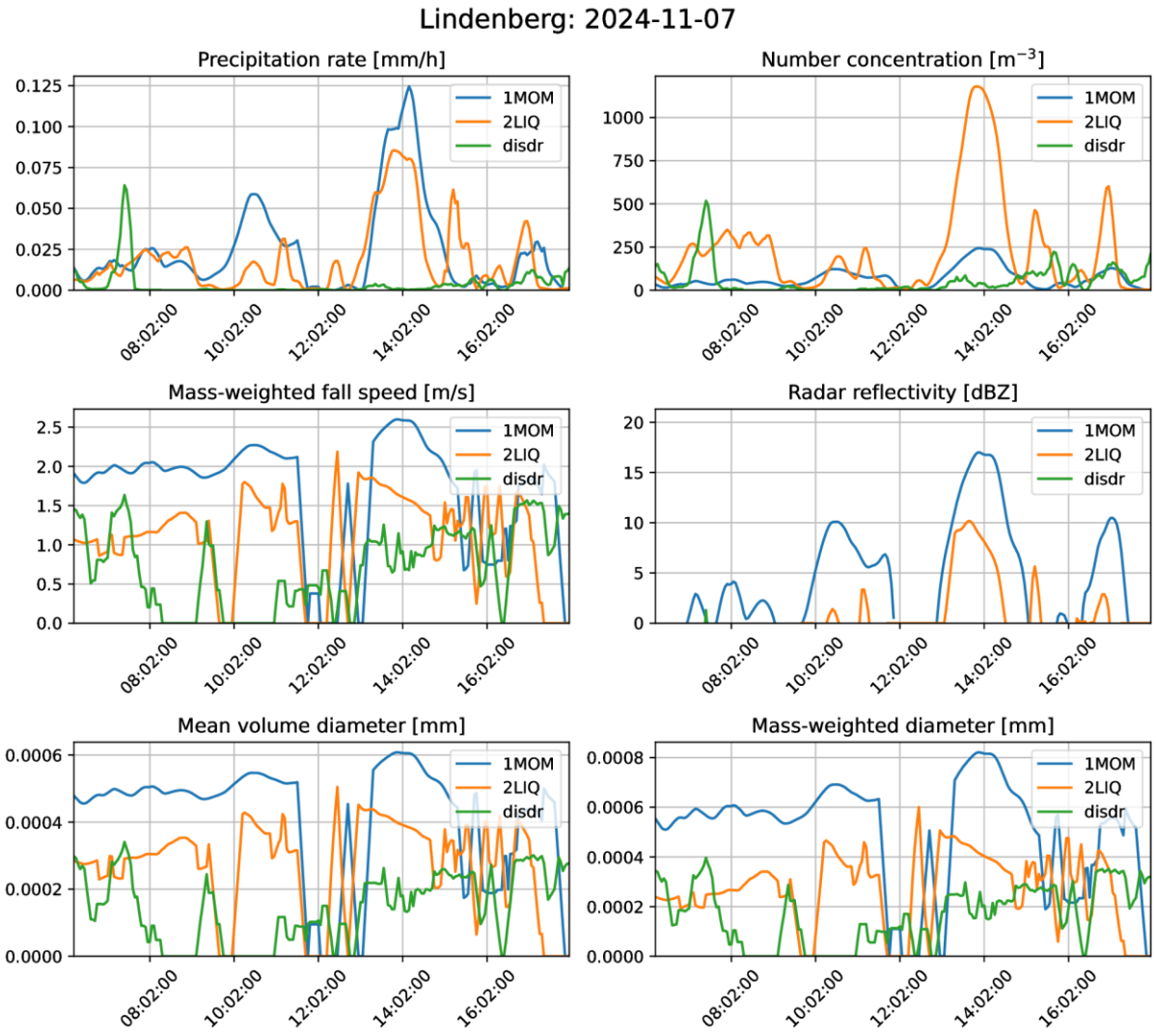


Fig. 3. Comparison of model to disdrometer data on 2024-11-07 at the Lindenberg station. 1MOM in blue, 2LIQ in orange, disdrometer in green.

A drizzle event is represented by a comparison for the Lindenberg station on 2024-11-07 from 06 to 18 UTC, shown in Fig. 3. The precipitation rate remains low throughout the time window, although it is somewhat overestimated by both model runs, especially by 1MOM. Despite the precipitation rate being overestimated by 1MOM, the number concentration remains very low even in phases with stronger precipitation, as confirmed by the too-high mean volume diameter and mass-weighted diameter, and by the radar reflectivity, suggesting that too many large drops occur in 1MOM. This bias is reduced with 2LIQ, and the diameters remain similar to those measured by the disdrometer. The maximum number concentration in 2LIQ is higher than that observed by the disdrometer. However, the precipitation rate is also higher, so the representation of the mean volume diameter and mass-weighted diameter stays closer to the disdrometer measurements in 2LIQ. The reduction of the mass-weighted fall speed in 2LIQ compared to 1MOM better matches the measurements.

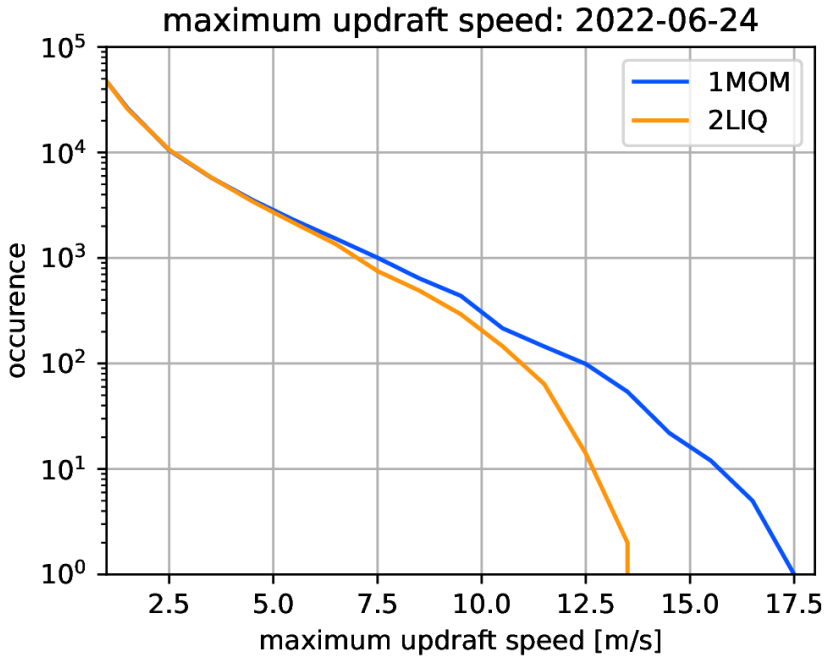


Fig. 4. Histogram of occurrence of the maximum vertical velocities in the vertical column on 2022-06-24 from 16 to 24 UTC, where a mesoscale convective system occurred.

Changes in microphysics does not only affect the surface precipitation accumulations but also the vertical structure of the atmosphere. One demonstration of these effects is shown in Fig. 4, which presents a histogram of the resolved vertical velocity over the passage of a mesoscale convective system on 2022-06-24. Only for this test, the deep convection parameterization was switched off to avoid two distinct vertical velocities, which might interact. Apparently, 2LIQ delivers slower updraft velocities than 1MOM for updraft velocities exceeding 5 $m \cdot s^{-1}$, while the frequency of vertical velocities between 1 and 5 $m \cdot s^{-1}$ is similar for this particular test.

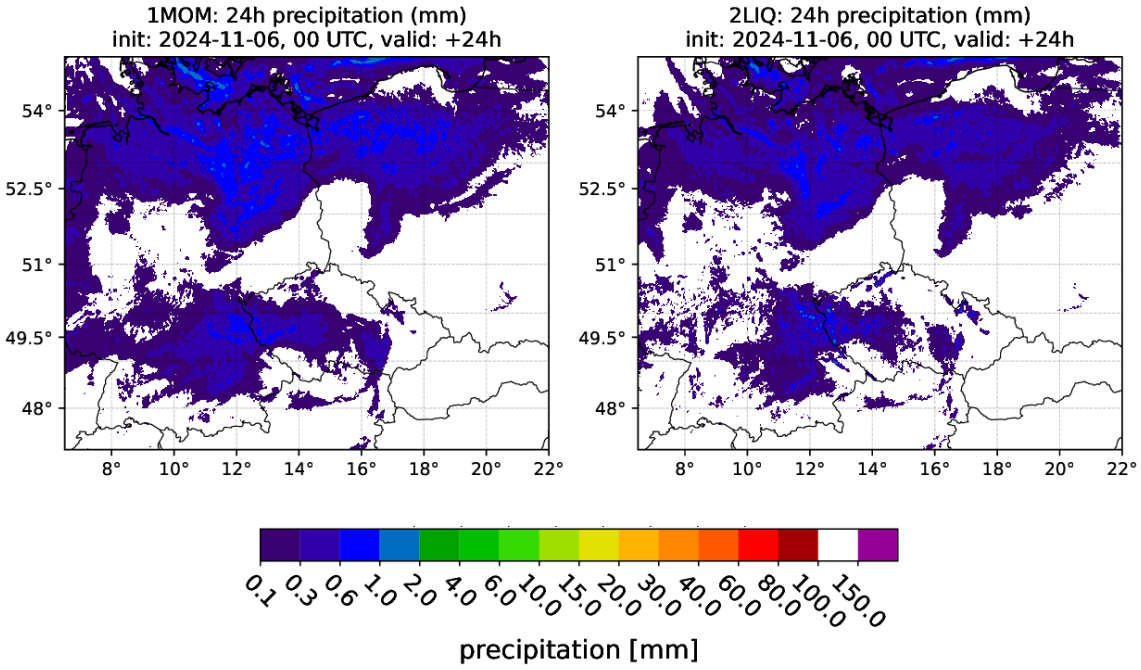


Fig. 5. 24h precipitation accumulation on 2024-11-06. Left: 1MOM, right: 2LIQ.

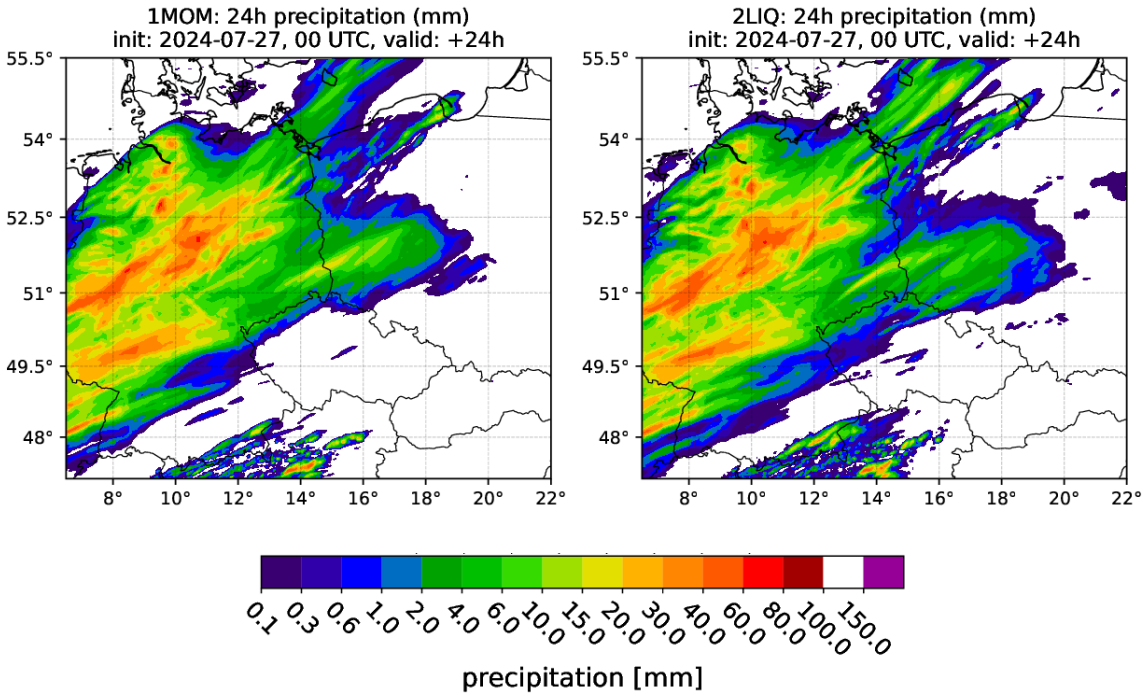


Fig. 6. 24h precipitation accumulation on 2024-07-27. Left: 1MOM, right: 2LIQ.

Finally, the precipitation patterns are somewhat altered. Fig. 5 shows a 24-hour precipitation accumulation from an autumn case on 2024-11-06. 2LIQ in this case reduces the area of light precipitation or drizzle. By contrast, Fig. 6 shows that the area of light precipitation amounts in a convective case is increased in 2LIQ. In addition, the area with precipitation exceeding 40 mm is also increased, but the absolute maximum is decreased.

Discussion

The comparison to the Thies Clima LPM disdrometers reveals several characteristics of the double-moment scheme. There is excessive size sorting at the onset of precipitation, producing too large drops and too high fall speeds compared to the disdrometer. The size sorting can be reduced by increasing the shape parameter of the gamma size distribution used for rain, as a higher shape parameter tightens the size spectra and makes the mass-weighted and number-weighted fall speeds more similar. On the other hand, 2MOM captures the peaking in number concentration in convective storms much better and also captures the transition to smaller droplets in the stratiform case. Finally, 2MOM shows a higher concentration of number particles during drizzle, thereby improving its representation.

The change in the scheme also modifies the updraft speeds, as the scheme delivers different fluxes of microphysical processes, especially through phase-changing processes such as melting or evaporation. Especially, it produces higher evaporation fluxes during heavy precipitation, creating a less pronounced temperature gradient and possibly weaker cold pools in selected cases (not shown), which might potentially weaken the dynamic forcing of updrafts.

The area of precipitation accumulation in a light autumn rain case on 2024-11-06 slightly reduced with the double-moment scheme. It is caused by the combination of autoconversion to rain, which is sensitive to the number concentration of cloud droplets, and the fact that more small particles are created at the given mass fraction with the double-moment scheme from the collision-coalescence process. Consequently, evaporation fluxes are higher, preventing precipitation from reaching the ground. Conversely, in a convection case, represented by 2024-07-27, most rain is produced by melting ice particles, so drops are often larger than in the single-moment scheme. Consequently, evaporation is lower, and the area of low precipitation accumulation is often larger. Finally, in the convective cores with the strongest rainfall, evaporation is again stronger than in the single-moment scheme.

Conclusion

The double-moment microphysics scheme is gradually developed in the ALARO model. Results from the double-moment microphysics scheme for rain and cloud water were shown. First, they were compared with disdrometer measurements, revealing strong size sorting during the onset of precipitation, better simulation of the transition to small droplets, and the ability of the new scheme to capture higher number concentrations in heavy rain and drizzle. Second, the vertical velocities in convective cases are reduced with the double-moment scheme mainly due to different evaporation fluxes. Third, the area of light precipitation in autumn is reduced, while it is increased in convective cases due to the sensitivity of the double-moment scheme to raindrop origin. A further development of the scheme is planned to mitigate its deficiencies.

Acknowledgments

The research was partially funded by the Technology Agency of the Czech Republic (grant no. SS02030040, PERUN).

References

Bozzo, A., et al., 2020. An aerosol climatology for global models based on the tropospheric aerosol scheme in the Integrated Forecasting System of ECMWF. *Geoscientific Model Development*, **13**(3), pp. 1007–1034. https://doi.org/10.5194/gmd-13-1007-2020

Daniel, M., et al., 2019. Benefits of explicit urban parameterization in regional climate modeling to study climate and city interactions. *Climate Dynamics*, **52**(5), pp. 2745–2764. https://doi.org/10.1007/s00382-018-4289-x

Deutscher Wetterdienst, Blahak, U., Tracksdorf, P., Antonoglou, N., 2025. Distrometer data of the Thies Laser Niederschlags Messer (LNM) since 2019 of about 150 German meteorological SYNOP stations [online]. *Zenodo*. https://doi.org/10.5281/zenodo.17157950.

Feingold, G., Heymsfield, A. J., 1992. Parameterizations of condensational growth of droplets for use in general circulation models. *Journal of Atmospheric Sciences*, **49**(23), pp. 2325–2342.

Němec, D., Brožková, R., Van Ginderachter, M., 2024. Developments of Single-Moment ALARO Microphysics Scheme with Three Prognostic Ice Categories. *Tellus*, **76**(1). https://doi.org/10.16993/tellusa.3464

Remedio, A. R., et al., 2019. Evaluation of new CORDEX simulations using an updated Köppen–Trewartha climate classification. *Atmosphere*, **10**(11), 726. https://doi.org/10.3390/atmos10110726

Sørland, S. L., et al., 2021. COSMO-CLM regional climate simulations in the Coordinated Regional Climate Downscaling Experiment (CORDEX) framework: a review. *Geoscientific Model Development*, **14**(8), pp. 5125–5154. https://doi.org/10.5194/gmd-14-5125-2021

Termonia, P., Fischer, C., Bazile, E., Bouyssel, F., Brožková, R., et al., 2018. The ALADIN System and its canonical model configurations AROME CY41T1 and ALARO CY40T1. *Geoscientific Model Development*, **11**, pp. 257–281. https://doi.org/10.5194/gmd-11-257-2018

Thompson, G., et al., 2008. Explicit forecasts of winter precipitation using an improved bulk microphysics scheme. Part II: Implementation of a new snow parameterization. *Monthly weather review*, **136**(12), pp. 5095–5115.